JACS
JOURNAL OF THE AMERICAN CHEMICAL SOCIETY
Communication
pubs.acs.org/JACS

In Situ Potentiodynamic Analysis of the Electrolyte/Silicon Electrodes Interface Reactions - A Sum Frequency Generation Vibrational Spectroscopy Study

Yonatan Horowitz,[§,†,‡] Hui-Ling Han,[§,†] Philip N. Ross,[†] and Gabor A. Somorjai*[,†,‡]

[†]Materials Sciences Division, Lawrence Berkeley National Laboratory, 1 Cyclotron Road, Berkeley, California 94720, United States
[‡]Department of Chemistry, University of California, Berkeley, California 94720, United States

Supporting Information

ABSTRACT: The key factor in long-term use of batteries is the formation of an electrically insulating solid layer that allows lithium ion transport but stops further electrolyte redox reactions on the electrode surface, hence solid electrolyte interphase (SEI). We have studied a common electrolyte, 1.0 M $LiPF_6$/ethylene carbonate (EC)/diethyl carbonate (DEC), reduction products on crystalline silicon (Si) electrodes in a lithium (Li) half-cell system under reaction conditions. We employed in situ sum frequency generation vibrational spectroscopy (SFG-VS) with interface sensitivity in order to probe the molecular composition of the SEI surface species under various applied potentials where electrolyte reduction is expected. We found that, with a Si(100)-hydrogen terminated wafer, a Si-ethoxy ($Si\text{-}OC_2H_5$) surface intermediate forms due to DEC decomposition. Our results suggest that the SEI surface composition varies depending on the termination of Si surface, i.e., the acidity of the Si surface. We provide the evidence of specific chemical composition of the SEI on the anode surface under reaction conditions. This supports an electrochemical electrolyte reduction mechanism in which the reduction of the DEC molecule to an ethoxy moiety plays a key role. These findings shed new light on the formation mechanism of SEI on Si anodes in particular and on SEI formation in general.

Lithium ion batteries are one of the most common forms of energy storage devices.[1,2] For electric vehicles where higher capacity is needed, the silicon based anodes are attractive candidates to replace graphite based anodes due to its theoretical capacity[3] of 4008 mAh/g. However, the Si lattice expands up to four times its volume,[4] which results in irreversible capacity loss and short cycling lifetime due to continued cracking and electrolyte consumption on the exposed Si surface.[5] The key factor in long-term use (cyclability and stability) of such devices is the formation of an electrically insulating layer that allows lithium ion transport at a reasonable rate while hindering electrolyte consumption on the Si anode surface, and is termed the solid electrolyte interphase (SEI).[5−7]

Previous studies from this laboratory have indicated that the nature of the electrolyte consuming reactions in lithium batteries is electrode material dependent.[8,9] Specifically, a study using ex situ infrared vibrational spectroscopy observed two different SEI compositions on Sn and Ni electrodes[10] even though the same electrolyte solution was used. Therefore, we may expect the electrolyte consuming reactions on Si may be unique to this surface and that the nature of the reactions may be a critical factor in determining the functioning of the surface layer formed, i.e. whether it functions as an SEI. The successful replacement of graphite by Si may require a detailed understanding of these surface[11] reactions and the ability to manipulate them by surface[12−14] or electrolyte modification[15] in particular by adding fluorinated EC to the electrolyte solution.[16,17]

A major obstacle in determining the SEI formation and composition is the practice of ex situ, post-cycling examination of lithiated samples that inevitably leads to loss of information. The need for a surface-sensitive technique that enables nondestructive and in situ analysis of the SEI chemistry such as SFG-VS[18] is crucial. SFG-VS was used successfully in previous electrochemical systems[19] on metallic electrodes (copper, gold)[20,21] as well as on cathode oxide materials ($LiCoO_2$).[22,23] We present the SFG-VS spectra of surface-electrochemical reactions in situ on a silicon anode and the differences between an oxide termination (SiO_2) and hydrogen one (Si−H).[24] We took the SFG-VS spectra under working conditions at three potential ranges. The voltagram shown in Figure 1 was taken with a Si(100)-hydrogen terminated surface and has three reduction peaks at ∼1.5, ∼0.5, and ∼0.10 V that are consistent with values reported in the literature.[25]

Therefore, we divide the potential range into three narrower ones. The first potential range (referred as ∼1 V) is at 1.1 to 0.8 V versus Li/Li^+ since no major reduction of EC molecules is expected. The second potential ranges between 0.65 V and 0.35 V (referred as ∼0.5 V) since EC molecules undergo several reduction reactions at this potential range. The third potential range was chosen between −0.05 to 0.10 V where lithiation is expected (referred as ∼0.1 V).

In Figure 2a, for the Si(100)-H electrode, we show the divided SFG spectrum after applying a 30 cycle cyclic-voltammetry (CV) potential near 1 V by the SFG in open circuit potential (OCP). Dividing the SFG spectra emphasizes the appearance of ethoxy group vibrational peaks (black line). The SFG from the Si/SEI is interferred with by the SFG

Received: October 5, 2015
Published: December 11, 2015

DOI: 10.1021/jacs.5b10333
J. Am. Chem. Soc. 2016, 138, 726−729

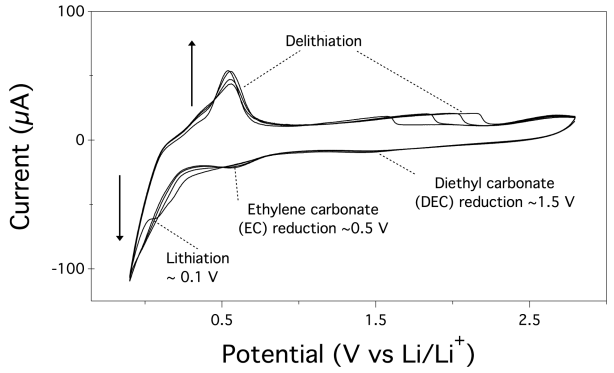

Figure 1. Three reduction peaks at a Si(100)-H anode of the electrolyte (1.0 M $LiPF_6$ in EC: DEC, 1:2 v/v) are presented in this CV plot. The reduction of DEC is around 1.5 V. The reduction of EC is about 0.5 V, and Li intercalation (lithiation) occurs around 0.10 V. Scan rate was 1 mV/s.

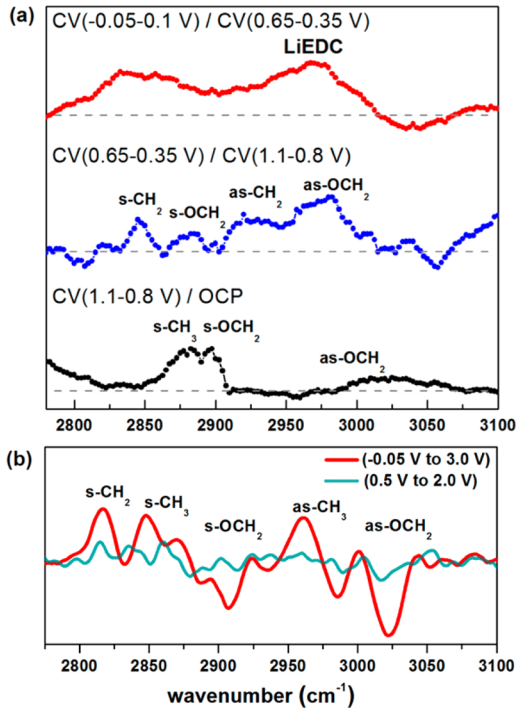

Figure 2. (a) We show the evolution of SFG signal under reaction conditions of crystalline silicon Si(100)-hydrogen terminated anode. The SFG spectra were taken at open circuit potential and after cyclic voltammetry at 1.1 V ↔ 0.8 V, 0.65 V ↔ 0.35 V, and 0.1 V ↔ −0.05 V. In order to emphasize the evolution of the Si-ethoxy peaks we divided the SFG spectra by their former potentials, as follows: $SFG_{1.1\ V \leftrightarrow 0.8\ V}$/OCP (black), $SFG_{0.65\ V \leftrightarrow 0.35\ V}/SFG_{1.1\ V \leftrightarrow 0.8\ V}$ (blue), and $SFG_{-0.05\ V \leftrightarrow 0.1\ V}/SFG_{0.65\ V \leftrightarrow 0.35\ V}$ (red). (b) The SFG profiles of crystalline silicon oxide Si(100) anode after cycling between 0.5 V ↔ 2.0 V (blue) and −0.05 V ↔ 3.0 V (red). All CVs were repeated for 30 cycles at a scan rate of 1 mV/s.

generated from the Si substrate.[26] We assume that if an intermediate species ethoxy radical[27,28] $^{\bullet}OCH_2CH_3$ (or anion, $^{-}OCH_2CH_3$)[29] is formed near the Si anode surface, it will react with Si−H to produce a $Si{-}OCH_2CH_3$ bond. This reaction cannot take place if a thick passivating oxide layer is present. In Figure 2a, we assigned the SFG peaks corresponding to Si-ethoxy bonds according to the work by Bateman et al.,[30] and SFG peaks relating to the various SEI components are as follows:[31,32] 2875 cm^{-1} ($s\text{-}CH_3$), 2895 cm^{-1} ($s\text{-}OCH_2$), and 2975 and 3025 cm^{-1} (both $as\text{-}OCH_2$).

After a 30 cycle CV at ~0.5 V (blue line), we observed peaks appearing at 2845 cm^{-1} ($s\text{-}CH_2$), 2895 cm^{-1} ($s\text{-}OCH_2$), 2920 cm^{-1} ($as\text{-}CH_2$), and 2975 and 3025 cm^{-1} ($as\text{-}OCH_2$). Most hydrocarbon molecules cannot be identified conclusively without using the whole IR spectrum. For example, poly-EC cannot be identified as such without using the asymmetric C−O−C band around 1100 cm^{-1} that is unique to poly-EC vs either DEC or EC. Therefore, we can only suggest our interpretation to the assigned products. Nevertheless, we attribute these observations to the EC molecules undergoing a reduction reaction into poly-EC and other ethyl carbonate species, as well as interact with DEC moieties. These reduction reactions are attributed to the beginning of the SEI formation.[33−35]

The SFG spectra taken after 30 CV between 0.1 V and −0.05 V (red line) show increasing peaks at 2850 cm^{-1}, and 2960 cm^{-1}, presumably due to the formation of lithium ethylene dicarbonate (LiEDC) and poly-EC. The peaks broaden due to surface deterioration after lithiation.

In the case of Si(100) oxide we did not observe any change at ~1 V; therefore, we extended the CV potential range. In Figure 2b, we compare the SFG spectra of the crystalline Si(100) oxide surface before and after lithiation. We performed a potential sweep in the range of 0.5 V to 2.0 V (blue profile) and between −0.05 V and 3.0 V. Each CV had 30 cycles, and the rate was 1 mV/s. The SFG profile of the first potential range (blue) has some SEI features but none that are related to a Si−O to $Si{-}OC_2H_5$ substitution reaction. After lithiation (red) prominent peaks appear and we assign them accordingly: 2817 cm^{-1} ($s\text{-}CH_2$), 2848 cm^{-1} ($s\text{-}CH_3$), 2895 and 2908 cm^{-1} (both $s\text{-}OCH_2$), 2960 cm^{-1} ($as\text{-}CH_3$), 2980 and 3022 cm^{-1} (both $as\text{-}OCH_2$).

We suggest that at ~1.0 V the ethoxy radical (or anion, $CH_3CH_2O^{-}$) reacts with acidic surface Si sites (Si−H) and substitutes the proton with an ethoxy group to produce a Si-ethoxy bond ($Si{-}OCH_2CH_3$). It has been proposed that all linear carbonates decompose via a linear alkyl anion (in our case the ethoxy anion $CH_3CH_2O^{-}$ featured in Scheme 1).[36]

We assume that the ethoxy radical/anion is the most likely species to chemically react with the oxide layer of the Si anode surface. The other electrolyte component, usually cyclic ether (ethylene carbonate in this study), cannot form an ethoxy radical. Therefore, even if EC is reduced before DEC it is the reduction of DEC to ethoxy that is significant in the anode surface substitution reaction.

In order to acquire a spectrum of a Si-ethoxy, we produced a Si-ethoxy wafer and the obtained SFG-VS spectrum of this sample is presented in Figure 3. The procedure is similar to the one reported by Michalak et al.[37,38] and is discussed in the Supporting Information (SI). The major peaks that we observed were at the following frequencies, and we have assigned them accordingly:[39] 2875 cm^{-1} ($s\text{-}CH_3$), 2895 cm^{-1} ($s\text{-}OCH_2$), 2912 cm^{-1} (*Fermi*), 2952 cm^{-1} ($as\text{-}CH_3$), and 2975 and 3040 cm^{-1} (both $as\text{-}OCH_2$). Obviously, the presence (or absence) of these peaks tells us if indeed Si-ethoxy sites are present.

According to previous calculations by Wang et al.[40] we assume that EC does not react with the Si−H surface as its intermediate anions swiftly reduce to LiEDC. Furthermore, we postulate that even if there is such bond formation, the surface concentration will be below our detection limit (less than a 0.1

DOI: 10.1021/jacs.5b10333
J. Am. Chem. Soc. 2016, 138, 726−729

Scheme 1. Proposed Formation Pathways of Electrolyte Reduction Products[a]

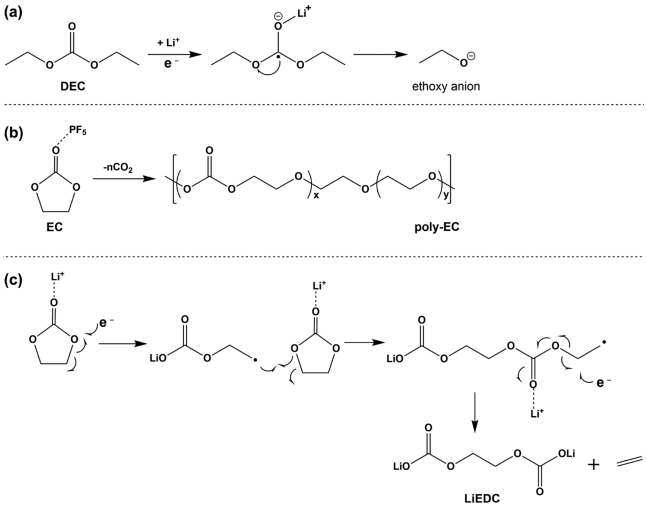

[a](a) Common to all DEC decomposition chemical pathways is the $CH_3CH_2O^-$ anion formation. In accordance with our findings this anion replaces the hydrogen terminated Si with an ethoxy group. (b) A proposed mechanism to the reduction of EC to poly-EC by a Lewis acid (PF_5).[9] (c) A suggested ring opening mechanism to form LiEDC.

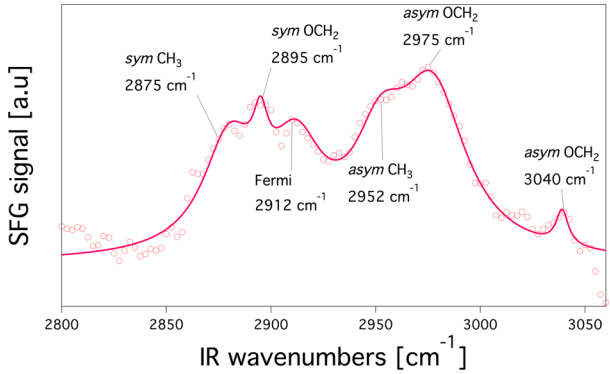

Figure 3. SFG profile of Si(100)-OC_2H_5. The peaks frequencies and their bond assignments are noted in the figure. Experimental data is presented in dots, and fitting with a Lorentzian peak function is shown as a solid line.

monolayer) due to steric effects blocking neighboring sites.[37,38] To further exclude the reduction of EC near the Si anode surface in the presence of $LiPF_6$ to form a Si compound, we have taken SFG spectra of 1.0 M $LiPF_6$:EC (diluted in *d*-THF to 3%, v/v) in contact with the Si(100)-H terminated wafer at two potential ranges (~1.0 V and ~0.5 V).

In Figure 4, we present the SFG intensity (i.e., the SFG of CV divided by the OCP spectrum) of EC on Si(100)-hydrogen terminated after cyclic voltammetry at 1.1 V ↔ 0.8 V (black) and 0.65 V ↔ 0.35 V (red). The SFG intensity profile at ~1 V has no detectible features as expected since EC reduction onset potential is at ~0.5 V. Once we lowered the applied potential to about 0.5 V (red curve), new peaks appeared that we assigned to poly-EC and LiEDC. Nevertheless, at ~1 V the absence of a peak at 2895 cm^{-1} corresponding to the s-OCH_2 group stretch associated with the Si-ethoxy formation reveals that only the reduction of DEC leads to Si-ethoxy formation. For poly-EC we assign the peaks at 2948 and 3000 cm^{-1}, and the peaks related to LiEDC are assigned at 2890, 2965, and 2980 cm^{-1}.[29]

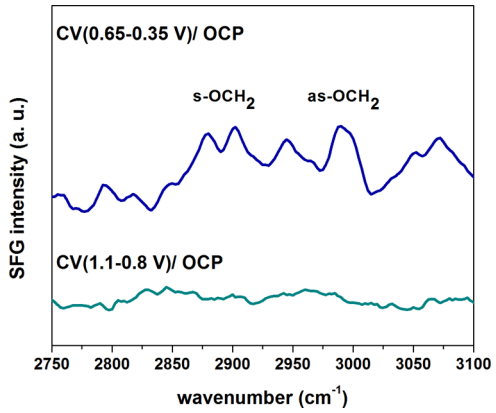

Figure 4. SFG intensity (i.e., divided by the OCP spectrum) of ethylene carbonate (EC) on Si(100)-hydrogen terminated after cyclic voltammetry at 1.1 V ↔ 0.8 V (cyan) and 0.65 V ↔ 0.35 V (blue).

In conclusion, by preforming SFG-VS together with CV we have observed that the Si-hydrogen terminated layer has been changed to Si-ethoxy (Si-OCH_2CH_3) at a potential close to 1.0 V only when DEC is present. The role of each electrolyte component (EC and DEC) was investigated separately. This substitution reaction at ~1.0 V did not take place when we changed the electrolyte to 1.0 M $LiPF_6$ in EC or when the Si(100)−O_x was used as the anode material. When we further reduced the potential to ~0.5 V only poly-EC and LiEDC formation was observed. Further in situ spectroelectrochemical (SFG-VS and CV) experiments of EC at reduction potentials of ~1.0 V and ~0.5 V suggest that it has been possibly reduced to poly-EC, but no Si-ethoxy termination was detected. Future SFG-VS in the C═O carbonyl stretch range and CV experiments are planned.

■ ASSOCIATED CONTENT

Supporting Information

The Supporting Information is available free of charge on the ACS Publications website at DOI: 10.1021/jacs.5b10333.

Additional information about the SFG apparatus, spectroelectrochemical half-cell set up, and general chemical description (PDF)

■ AUTHOR INFORMATION

Corresponding Author

*E-mail: Somorjai@Berkeley.edu.

Author Contributions

[§]These authors contributed equally.

Notes

The authors declare no competing financial interest.

■ ACKNOWLEDGMENTS

This work was supported by the Assistant Secretary for Energy Efficiency and Renewable Energy, Office of Freedom CAR and Vehicle Technologies of the U.S. Department of Energy under Contract No. DE-AC02 O5CH1123. The SFG instrumentation was purchased with funding from the Director, Office of Basic Energy Sciences, Materials Science and Engineering Division of the U.S. Department of Energy. This work was also funded through a grant from Honda Research Institute. The authors also wish to thank E. Edri and N. Kornienko for their technical insights and support.

DOI: 10.1021/jacs.5b10333
J. Am. Chem. Soc. 2016, 138, 726−729

REFERENCES

(1) Goodenough, J. B.; Park, K.-S. *J. Am. Chem. Soc.* **2013**, *135*, 1167.
(2) Kraytsberg, A.; Ein-Eli, Y. *Adv. Energy Mater.* **2012**, *2*, 922.
(3) Obrovac, M. N.; Krause, L. J. *J. Electrochem. Soc.* **2007**, *154*, A103.
(4) Liu, N.; Lu, Z.; Zhao, J.; McDowell, T. M.; Lee, H.-W.; Zhao, W.; Cui, Y. *Nat. Nanotechnol.* **2014**, *9*, 187.
(5) Xu, K.; von Cresce, A. V. *J. Mater. Chem.* **2011**, *21*, 9849.
(6) Peled, E. *J. Electrochem. Soc.* **1979**, *126*, 2047.
(7) Peled, E.; Golodnitsky, D.; Ardel, G. *J. Electrochem. Soc.* **1997**, *144*, L208.
(8) Ross, P. N. *Catal. Lett.* **2014**, *144*, 1370.
(9) Shi, F.; Ross, P. N.; Zhao, H.; Liu, G.; Somorjai, G. A.; Komvopoulos, K. *J. Am. Chem. Soc.* **2015**, *137*, 3181.
(10) Shi, F.; Zhao, H.; Liu, G.; Ross, P. N.; Somorjai, G. A.; Komvopoulos, K. *J. Phys. Chem. C* **2014**, *118*, 14732.
(11) Zhao, J.; Lu, Z.; Wang, H.; Liu, W.; Lee, H.-W.; Yan, K.; Zhuo, D.; Lin, D.; Liu, N.; Cui, Y. *J. Am. Chem. Soc.* **2015**, *137*, 8372.
(12) Philippe, B.; Dedryvère, R.; Allouche, J.; Lindgren, F.; Gorgoi, M.; Rensmo, H.; Gonbeau, D.; Edström, K. *Chem. Mater.* **2012**, *24*, 1107−1115.
(13) Schroder, K. W.; Dylla, A. G.; Harris, S. J.; Webb, L. J.; Stevenson, K. J. *ACS Appl. Mater. Interfaces* **2014**, *6*, 21510−21524.
(14) Schroder, K.; Alvarado, J.; Yersak, T. A.; Li, J.; Dudney, N.; Webb, L. J.; Meng, Y. S.; Stevenson, K. J. *Chem. Mater.* **2015**, *27*, 5531−5542.
(15) Li, S. R.; Sinha, N. N.; Chen, C. H.; Xu, K.; Dahn, J. R. *J. Electrochem. Soc.* **2013**, *160*, A2014.
(16) Nie, M.; Abraham, D. P.; Chen, Y.; Bose, A.; Lucht, B. L. *J. Phys. Chem. C* **2013**, *117*, 13403−13412.
(17) Xu, C.; Lindgren, F.; Philippe, B.; Gorgoi, M.; Björefors, F.; Edström, K.; Gustafsson, T. *Chem. Mater.* **2015**, *27*, 2591−2599.
(18) Shen, Y. R. *Nature* **1989**, *337*, 519.
(19) Romero, C.; Baldelli, S. *J. Phys. Chem. B* **2006**, *110*, 11936.
(20) Mukherjee, P.; Lagutchev, A.; Dlott, D. D. *J. Electrochem. Soc.* **2012**, *159*, A244.
(21) Nicolau, B. G.; Garcıá-Rey, N.; Dryzhakov, B.; Dlott, D. D. *J. Phys. Chem. C* **2015**, *119*, 10227.
(22) Liu, H.; Tong, Y.; Kuwata, N.; Osawa, M.; Kawamura, J.; Ye, S. *J. Phys. Chem. C* **2009**, *113*, 20531.
(23) Yu, L.; Liu, H.; Wang, Y.; Kuwata, N.; Osawa, M.; Kawamura, J.; Ye, S. *Angew. Chem., Int. Ed.* **2013**, *52*, 5753.
(24) Kolasinski, K. W. *Phys. Chem. Chem. Phys.* **2003**, *5*, 1270.
(25) Schroder, K. W.; Celio, H.; Webb, L. J.; Stevenson, K. J. *J. Phys. Chem. C* **2012**, *116*, 19737.
(26) Malyk, S.; Shalhout, F. Y.; O'Leary, L. E.; Lewis, N. S.; Benderskii, A. V. *J. Phys. Chem. C* **2013**, *117*, 935.
(27) Ein-Eli, Y. *Electrochem. Solid-State Lett.* **1999**, *2*, 212.
(28) Zhang, X.; Kostecki, R.; Richardson, T. J.; Pugh, J. K.; Ross, P. N. *J. Electrochem. Soc.* **2001**, *148*, A1341.
(29) Haregewoin, A. M.; Leggesse, E. G.; Jiang, J.-C.; Wang, F.-M.; Hwang, B.-J.; Lin, S.-D. *Electrochim. Acta* **2014**, *136*, 274.
(30) Bateman, J. E.; Eagling, R. D.; Horrocks, B. R.; Houlton, A. *J. Phys. Chem. B* **2000**, *104*, 5557.
(31) Zhuang, G. V.; Xu, K.; Yang, H.; Jow, T. R.; Ross, P. N. *J. Phys. Chem. B* **2005**, *109*, 17567.
(32) Xu, K.; Zhuang, G. V.; Allen, J. L.; Lee, U.; Zhang, S. S.; Ross, P. N.; Jow, T. R. *J. Phys. Chem. B* **2006**, *110*, 7708.
(33) Chan, C. K.; Peng, H.; Liu, G.; McIlwrath, K.; Zhang, X. F.; Huggins, R. A.; Cui, Y. *Nat. Nanotechnol.* **2008**, *3*, 31.
(34) Peng, K.; Jie, J.; Zhang, W.; Lee, S.-T. *Appl. Phys. Lett.* **2008**, *93*, 033105.
(35) Baranchugov, V.; Markevich, E.; Pollak, E.; Salitra, G.; Aurbach, D. *Electrochem. Commun.* **2007**, *9*, 796.
(36) Haregewoin, A. M.; Shie, T.-D.; Lin, S.-D.; Hwang, B.-J. *ECS Trans.* **2013**, *53*, 23.
(37) Michalak, D. J.; Amy, S. R.; Aureau, D.; Dai, M.; Estève, A.; Chabal, Y. J. *Nat. Mater.* **2010**, *9*, 266.
(38) Michalak, D. J.; Amy, S. R.; Aureau, D.; Estève, A.; Chabal, Y. J. *J. Phys. Chem. C* **2008**, *112*, 11907.
(39) Gomes, J. F.; Bergamaski, K.; Pinto, M. F.S.; Miranda, P. B. *J. Catal.* **2013**, *302*, 67.
(40) Wang, Y.; Nakamura, S.; Ue, M.; Balbuena, P. B. *J. Am. Chem. Soc.* **2001**, *123*, 11708−11718.

DOI: 10.1021/jacs.5b10333
J. Am. Chem. Soc. 2016, 138, 726−729